A Theoretical Model of a Plant Antifreeze Protein from *Lolium perenne*

Michael J. Kuiper,* Peter L. Davies,*† and Virginia K. Walker*
Departments of *Biology and †Biochemistry, Queen's University, Kingston, Ontario K7L 3N6, Canada

ABSTRACT Antifreeze proteins (AFPs), found in certain organisms enduring freezing environments, have the ability to inhibit damaging ice crystal growth. Recently, the repetitive primary sequence of the AFP of perennial ryegrass, *Lolium perenne*, was reported. This macromolecular antifreeze has high ice recrystallization inhibition activity but relatively low thermal hysteresis activity. We present here a theoretical three-dimensional model of this 118-residue plant protein based on a β-roll domain with eight loops of 14–15 amino acids. The fold is supported by a conserved valine hydrophobic core and internal asparagine ladders at either end of the roll. Our model, which is the first proposed for a plant AFP, displays two putative, opposite-facing, ice-binding sites with surface complementarity to the prism face of ice. The juxtaposition of the two imperfect ice-binding surfaces suggests an explanation for the protein's inferior thermal hysteresis but superior ice recrystallization inhibition activity and activity when compared with fish and insect AFPs.

INTRODUCTION

Antifreeze proteins (AFPs) have the ability to bind to ice crystals and restrict their growth, enabling certain organisms to survive under freezing conditions that would otherwise prove fatal. Although exact details of the antifreeze mechanism have not been established, it is widely regarded that AFPs require some structural complementarity with ice to adsorb to its surface. AFP adsorption results in a noncolligative freezing point depression as ice is then forced to grow in the spaces between adsorbed molecules, increasing local ice surface curvature (Raymond and DeVries, 1977). In the temperature gap between the melting and freezing points of ice in the presence of AFPs, (the range of which is known as the thermal hysteresis (TH)), ice expansion along these curved fronts is thermodynamically unfavorable. The extent of the TH is a measure of AFP activity, which is a function of both the AFP type and concentration. AFPs also inhibit the recrystallization of ice, a process whereby the migration of ice grain boundaries creates larger ice crystals at the expense of smaller ones. Recrystallization is thermodynamically favorable because it minimizes the ice interfacial surface area between ice crystals.

AFPs have been identified from a wide variety of sources including polar fish, insects, bacteria, and plants. Some AFPs have been structurally characterized, revealing a remarkably diverse range of protein folds. Of the current five distinct types of AFPs isolated from polar fish, three have solved structures. Type I AFPs from flounder and sculpin are amphiphilic, single α-helices of ~30 to 50 residues (Sicheri and Yang, 1995), with putative ice-binding threonine residues repeated every 11 amino acids along the length of the helix. Type II AFPs found in sea raven, smelt, and herring are ~125 residues long and have homology to C-type lectins with a mixed structure containing two α-helices and two β-sheets (Gronwald et al., 1998). Type III AFPs, isolated from Arctic and Antarctic eel pouts, are globular proteins of ~65 residues but with a flat ice-binding face (Jia et al., 1996; Sönnichsen et al., 1996). The structures of insect AFPs from the spruce budworm moth (*Choristoneura fumiferana*) and the mealworm beetle (*Tenebrio molitor*) have recently been characterized as parallel β-helices in the left- and right-handed orientations, respectively (Graether et al., 2000; Liou et al., 2000). At physiological concentrations, the TH activity of fish AFPs is typically ~1–1.5°C, whereas insect AFPs can produce ~5°C of activity.

Plant AFPs have been isolated from species such as bittersweet nightshade (*Solanum dulcamara*), winter rye (*Secale cereale*), and carrot (*Daucus carota*). They have a relatively weak TH activity of ~0.1–0.5°C (Urrutia et al., 1992; Antikainen and Griffith, 1997; Worrall et al., 1998). The perennial ryegrass *Lolium perenne*, like other freeze-tolerant plants, can withstand some freezing of cellular structure. In contrast, freeze-intolerant plants suffer lethal freeze damage, including cytoplasmic dehydration and rupture of the cellular membranes, and are not reported to produce AFPs (Levitt, 1980). In freeze-tolerant plants, differences in lipid membrane composition allow for cold temperature stabilization of membranes that prevent cellular leakage (Steponkus et al., 1993). Freeze-tolerant plants also use a range of small molecular weight solutes such as simple sugars to further stabilize membrane structures or combat freeze-induced osmotic imbalances (Thomashow, 1998). In addition, AFPs are produced by some freeze-tolerant plants, but because of their low TH activity, it has been speculated that their main function is to inhibit ice recrystallization rather than depress the freezing point of plant fluids (Urrutia et al., 1992).

Recently, a 118-residue AFP with superior ice recrystallization inhibition activity was isolated from the ryegrass and was found to contain a 7-residue repeating motif of consensus sequence X X N X V X G (Sidebottom et al.,

Received for publication 6 June 2001 and in final form 27 August 2001.
Address reprint requests to Dr. Virginia K. Walker, Queen's Universuty, Department of Biology, Kingston, Ontarion K7L 3N6 Canada. Tel.: 613-533-6123; Fax: 613-533-6617; E-mail: walkervk@biology.queensu.ca.

0006-3495/01/12/3560/06 $2.00

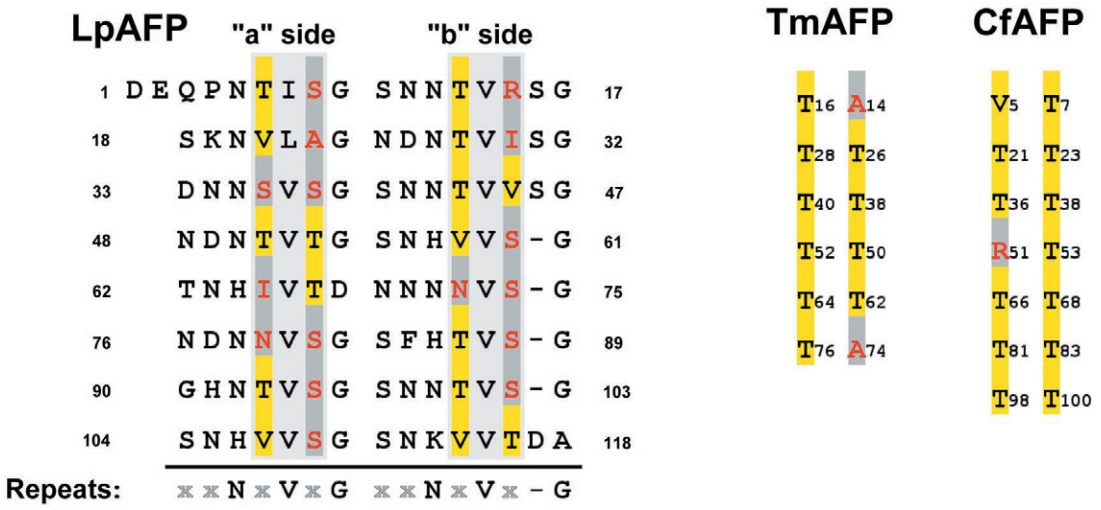

FIGURE 1 Comparison of the putative ice binding surfaces (shaded, boxed regions) of *L. perenne* AFP to representative parallel β-sheet ice binding surfaces of insect AFPs from *Tenebrio molitor* (clone 4–9; Liou et al., 1999) and *Choristoneura fumiferana* (isoform 10; Doucet et al., 2000). In the ice-binding regions, outward-facing threonine and space-filling similar valine residues are shaded yellow whereas other residues projecting into the solvent are shaded gray. The complete sequence of the LpAFP is shown to the left, aligned to highlight the repeating sequence (X X N X V X G).

2000). Guided by our knowledge of the structures of fish and insect AFPs and the protein's primary sequence, we have constructed a three-dimensional (3-D) model of the *L. perenne* (Lp) AFP, using a right-handed β-roll domain as the main structural feature. The model has some similarity to the β-helical insect AFP structures. It predicts two ice-binding sites, one on either side of the AFP, with complementarity to the prism face of ice. This unusual duplication of putative ice-binding sites on opposite sides of the protein may explain the superior ice recrystallization inhibition activity of LpAFP.

The LpAFP model: rationale and construction

Aligning the LpAFP sequence in two columns of approximately seven-amino acid repeats reveals the X X N X V X G motif (Fig. 1) and suggests a repetitive 3-D structure. Fourier transform infrared spectrophotometry measurements, as reported by Sidebottom et al. (2000) showed a high content of solvent-exposed β-sheet. This, in addition to ice-etching studies indicating LpAFP's binding preference for the prism face of ice, suggested that the plant AFP may have some structural similarity to the recently characterized insect AFPs, which also have repetitive sequence, a high β-sheet content, and a preference for prism face ice-binding (Graether et al., 2000; Liou et al., 2000). Prism face preference for the insect AFPs is thought to occur because the 4.5-Å spacing between adjacent β-strands of the ice-binding surface is the same as the spacing between adjacent, identically oriented ice lattice positions along the *a*-axis of the prism face of ice. We hypothesized that LpAFP adopts a similar β-helix conformation with the seven-amino-acid repeating motif making up the sides of the β-helix. If three repeating motifs are required to make one complete loop of a β-helix, similar to those proposed for pentapeptide repeats found in some bacterial proteins (Bateman et al., 1998), then the cross-section of the β-helix would be triangular as in the spruce budworm AFP (Graether et al., 2000). This initial conformation was constructed with the conserved valine residues facing the center of the β-helix to provide a hydrophobic core for structural stability. It was soon realized that this conformation was unlikely, as the conserved small valine residues left large spaces in the center of the β-helix. Indeed, inspection of the crystal structure of a similar triangular cross-sectioned β-helical domain of carbonic anhydrase from the bacteria *Methanosarcina thermophila* (Kisker et al., 1996), showed that of 22 residues participating in the hydrophobic core, only 9 are valine, 1 is alanine, whereas bulkier residues, including 9 isoleucine and 3 leucine, make up the remainder.

A second model was then constructed using only two repeat motifs per loop (Fig. 2). This arrangement brings the conserved valine residues together to form a tight hydrophobic core sandwiched between two parallel β-sheets. This structure is reminiscent of the β-roll domain of alkaline protease from *Pseudomonas aeruginosa*, where two 9-amino-acid repeat units fold to form a β-helix loop (Baumann et al., 1993). This protease β-roll domain is further stabilized by calcium ions bound within the turn motifs. Recently, an isolated β-roll domain was synthesized and shown to fold in the presence of calcium ions and polyethylene glycol (Lilie et al., 2000). Our model was loosely based on this right-handed β-roll domain, although each β-helix loop is shorter by four residues and lacks the calcium-binding regions.

TABLE 1 Secondary structure prediction of *Lolium perenne* AFP*

LpAFP sequence (10 · 20 · 30 · 40 · 50 · 60 · 70 · 80 · 90 · 100 · 110)	Prediction method
DEQP**NTIS**GSN**NTVR**SGSK**NVLA**GND**NTVI**SGDN**NSVS**GSN**NTVV**SGND**NTVT**GSN**HVVS**GTN**HIVT**DNN**NNVS**GND**NNVS**GSF**HTVS**GGH**NTVS**GSN**NTVS**GSN**HVVS**GSN**KVVT**DA	
ccccccccccccEEEccccEEEEccccEEEEcccccccccccEEEEcccccEEEcccEEccccEEEEcccccccccccccccEEEEEEcccEEEEccccccccccEEEEcccEEEEEc	GOR4 (1)
cccccccccccccccccccEEEEccccEEEEcccccccccccEEEEcccccEccccEEEEcccEEEEccccccccccccccccEEEEccccccccccccccccccEEEccccEEEEcc	HNN (2)
ccccccEtccccEEEttccEEEEtcccEEEEcccccccccccEEEEcccccEEcccEEEEtccEEEEcttcccccccccccccEEEEcccccEEEccccccccccEEEEtcccEEEEt	SOMPA (3)
------------EE------------EEEE----EEEE---EEEE----EEEE----EE----EEE-----EEE---EEE----EEEE---EEEE----EEEEEEEEE----EEEE--	JPred (4)
----EEE--EEE-----EEEEEE----EEEE----EEEEE--EEEEE--EEEEEEEEEEE--EEEEEE---EEE----EEE---EEE---EEEEE----EEE---EEEEE-EEEEEE-	PredictProtein (5)
ccccccccccccccccccccEEEccccEEEEcccccccccccEEEEccccEEEcccEEEEcccEEEEccccccccccccccccEEEEcccccccccccccccccccEEEcccEEEccc	PSIPred (6)
Legend: E = β-strands C = random coil t = turn	

*Comparison of predicted secondary structure to that of the *Lolium perenne* AFP model. Gray shaded regions represent ice binding β-strand regions in the LpAFP model. (1) (Garnier *et al.*, 1996); (2) (Guermeur *et al.*, 1999); (3) (Geourjon and Deléage, 1995); (4) (Cuff *et al.*, 1998); (5) (Rost, 1996); (6) (Jones, 1999).

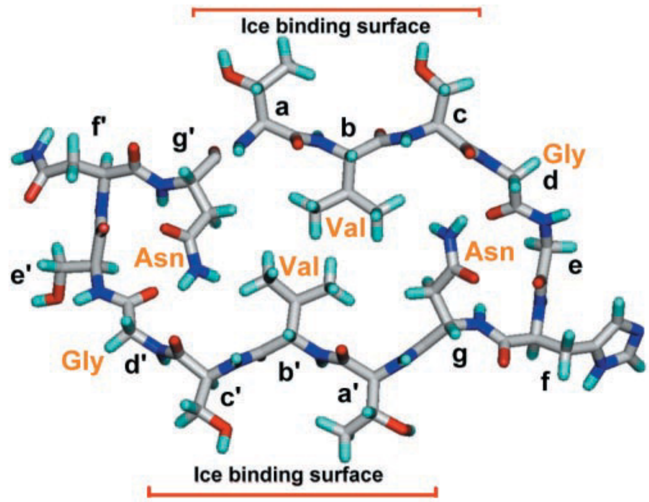

FIGURE 2 Cross-section of LpAFP model showing positions of conserved residues and the putative ice binding surfaces. Two repeat motifs, (X X N X V X G), are needed for each loop, each corresponding to repeat labeled *a-g* and *a′-g′*.

The repeating motif of the LpAFP seems well suited to fold in a β-roll. The conserved internal valine residues form a valine stack along the center of the β-roll (Fig. 2). The uniformity and small size of the valine residues in the core allows for the parallel β-sheets on each side of the β-roll to pack closely and evenly together. Only residues Ile^7 and Leu^{22} are the exceptions to the conserved valine core. They are positioned at the beginning of the β-helix, where the loops have an extra residue, and hence their additional bulk does not disrupt the valine packing significantly. The conserved glycine residues occur at the turns allowing the β-strands to bend into the β-roll. The relatively well conserved asparagine residues also occur at the turns, and are directed internally to form an asparagine ladder similar to those observed in many β-helical lyases (Jenkins et al., 1998). The asparagine residues on adjacent β-strand loops form hydrogen bonds to one another through the amide and carbonyl functional groups. Additional hydrogen bonds between the asparagine amide and the peptide bond carbonyl of adjacent β-strands further stabilize the turn motif. Histidine residues at positions 57, 64, 85, and 106 are aligned internally within the β-roll asparagine ladder and seem to be well tolerated as they form hydrogen bonds with asparagine residues on adjacent β-strands (Fig. 1).

Three additional serine residues at positions 16, 31, and 46, in the first three loops of the model are readily accommodated by introducing a slight bulge on one side of the β-roll structure toward the N terminus. The remaining portion of the model has a very regular backbone structure forming two flat β-sheets with spacing of side chain residues complementary to that of the primary prism face of ice. The N terminus of the LpAFP model is stabilized by strong salt bridge interactions between arginine 15 and the residues

aspartic acid 1 and glutamic acid 2. Another salt bridge occurs between aspartic acid 33 and lysine 19.

Six potential N-linked glycosylation sites exist at asparagines 11, 34, 41, 72, 79, and 98 where the asparagine residue is part of a Asn-X-Ser/Thr N-linked glycosylation motif, in which X can be any residue except proline. All asparagine residues of the potential glycosylation sites are directed outward from the β-helix core. Glycosylation occurring at positions 11, 34, 41, and 98 can be directed perpendicular to the putative ice-binding site and would thus be unlikely to interfere with the ice recognition mechanism. However, if glycosylation were to occur at positions 72 and 79, which are part of the proposed ice-binding surfaces, these additions would presumably interfere with ice adsorption.

The amino acid sequence of the LpAFP was used in six secondary structure prediction algorithms. Of the predicted β-strand regions, 86% occurred within the modeled β-sheet regions of the putative ice-binding faces (Table 1). Overall, the predicted secondary structure was generally consistent with our LpAFP model, with short periodic stretches of β-strand aligning with the β-strand regions of the two ice-binding surfaces.

The structural validity of the model was checked using the program PROCHECK v3.5 (Laskowski et al., 1993) which showed that >98% of nonglycine residues occupied the most favored regions of a Ramachandran plot with favorable side chain conformations. Only asparagine 68, although occupying allowable ϕ/ψ angles, slightly distorts the local structure, straining to fit in a position normally occupied by glycine. (Model coordinates are deposited in the protein data bank, i.d. number: 1I3B).

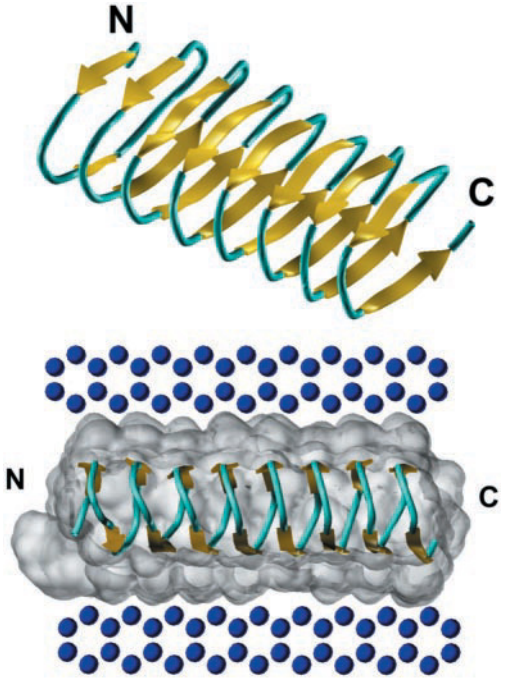

FIGURE 3 (*Top*) β-Helix structure of the LpAFP theoretical structure, showing two parallel β-sheet regions of putative ice-binding surfaces in yellow. (*Bottom*) LpAFP aligned along the prism face of ice (parallel to the *a*-axis) with van der Waals surfaces displayed on the protein to highlight the surface complementarity to ice water molecules (*blue spheres*). An additional row of ice water molecules are positioned along the top of the LpAFP van der Waals surface to highlight the dual-sided ice complementarity. Each successive loop matches the 4.5-Å repeat spacing of the ice along the prism face.

Putative ice-binding surfaces and implications for activity

LpAFP has two putative ice-binding surfaces, one on either side of the flat parallel β-sheet roll. They each consist of two ranks of aligned, solvent-accessible residues similar to those in insect AFPs but with more amino acid substitutions (Fig. 1). In insect AFP ice-binding surfaces, the two ranks of solvent-accessible residues are mostly threonine with the occasional substitution by isoleucine, arginine, valine, serine, and alanine (Liou et al., 1999; Doucet et al., 2000; Andorfer and Duman, 2000). On the LpAFP ice-binding surfaces, the most abundant residue is also threonine (11 of 32), followed by serine and valine, which are potentially good functional and structural matches for threonine. The remaining 6 of the 32 are alanine, arginine, asparagine, and isoleucine. Because the parallel β-sheet backbone scaffolds for the putative ice-binding surfaces are similar to those observed in the insect AFPs, the interresidue spacing is also similar, with ~4.5 Å between adjacent β-strands and 7.4 Å between residues separated by two positions on the same β-strand. This residue spacing arrangement in insect AFPs is thought to facilitate binding through a complementary surface match to the prism ice surface which repeats every 4.52 Å along the *a*-axis and every 7.35 Å along the *c*-axis. The putative ice-binding sites of the LpAFP have surface complementarily to the prism face of ice as shown by the van der Waals surface representation in Fig. 3.

Although there is good ice surface complementarity with the LpAFP model, this plant AFP has a rather poor TH activity of only 0.1°C in water and 0.45°C in 30% sucrose (Sidebottom et al., 2000). In contrast, AFPs from freeze-intolerant insects have reported activities in the range of 5–6°C (Graham et al., 1997; Tyshenko et al., 1997; Li et al., 1998). The main function of the LpAFP, however, seems to be the inhibition of ice recrystallization to confer freeze-tolerance to the plant. At temperatures just below the melting point, ice recrystallization can be quite pronounced, with large crystals forming at the expense of smaller crystals. AFPs have the ability to inhibit this ice boundary migration, by adsorbing at the ice interface, making boundary movement energetically unfavorable (Knight et al., 1995). For an ice boundary to free itself from adsorbed AFP, it must first increase the boundary interface to migrate around the protein. This is a thermodynamically unfavor-

able process, as the free energy of the system is lowered by decreasing the boundary interfaces and, conversely, raised by increasing the boundary interface. Thus, the ice interfaces are effectively inhibited from movement by adsorbed proteins. AFPs exert ice recrystallization inhibition activity at orders-of-magnitude lower concentrations than those required for measurable TH activity. LpAFP seems to be particularly effective at ice recrystallization inhibition, functioning at concentrations 200 times lower (<10 μg/ml) in molar terms than type III AFP from ocean pout, and yet, with a seemingly paradoxical 10 times lower TH activity when compared with the fish AFP (Sidebottom et al., 2000).

Based on the model for the 3-D structure of LpAFP, we suggest an explanation for the apparent converse relationship between TH and recrystallization inhibition of AFPs. A reduction in TH activity is explained by substitution of threonines on the ice-binding surfaces. Replacement of two or more threonines in type I AFP by the space-filling equivalent residue, valine, reduced TH activity to ~80% of original activity (Chao et al., 1997; Haymet et al., 1998; Zhang et al., 1998), however substitution by serine caused a significant ($>70\%$) loss in TH. A similar loss of TH activity was observed when the insect ice-binding site threonine residues were replaced by larger side chain leucine residues (Graether et al., 2000). Both ice-binding sites of LpAFP have these types of substitutions that would prevent the optimal TH activity seen with insect AFPs, presumably by reducing surface complementarity to the ice surface and hence the strength of interaction. Reduction in TH activity is beneficial for freeze-tolerant organisms such as *L. perenne* because it would avoid significant supercooling that could eventually lead to damaging, rapid growth of ice at lower temperatures; controlled freezing is preferred. Such a freeze-tolerant strategy for plants makes sense, as there is no advantage for the plant to remain unfrozen under freezing conditions if there is no environmental liquid water present to maintain normal physiological functions.

We suggest that the key attribute for LpAFP's enhanced ice recrystallization inhibition activity is the presence of ice-binding sites on opposite sides of the β-roll. These parallel sites could simultaneously bind and stabilize the ice fronts between two adjacent ice grains. Such a bifunctional AFP would be ideally positioned to stop ice boundary migration, far more so than an AFP with a single ice-binding site. In essence, the molecule may act as interfacial "glue," somewhat analogous to double-sided adhesive tape (Figs. 2 and 3).

The theoretical 3-D β-roll model, presented here, of an AFP from the perennial ryegrass, *L. perenne*, is consistent with spectrometric evidence suggesting solvent exposed β-sheet structure. The two putative ice-binding surfaces, optimally spaced for complementary binding to the ice prism face are not only consistent with ice etching results, but may also help explain the relative low TH and superior ice recrystallization inhibition activity of this protein.

MATERIALS AND METHODS

All modeling was performed using SYBYL molecular modeling package (version 6.4, Tripos Associates, St. Louis, MO) operating on a Silicon Graphics O_2 workstation. The biopolymer module was used to manually construct the LpAFP protein. The model was geometrically optimized using a combination of constraints and minimization routine. All modeling used the Tripos force field, Gastiger-Marsili derived charges, and a distant-dependent dielectric constant. Final minimization iterations were performed until the gradient cutoff value between successive iterations was <0.05 kcal/mol. The translated protein sequence of *L. perenne* obtained from GenBank, (accession number AJ277399), was used in secondary structure prediction algorithms accessible from the ExPASy molecular biology server (http://www.expasy.ch/) to check for structural consensus with the model. The algorithms used were: GOR IV (Garnier et al., 1996), HNN (Guermeur et al., 1999), SOMPA (Geourjon and Deléage, 1995), JPred (Cuff et al., 1998), PredictProtein (Rost, 1996), and PSIPred (Jones, 1999). The program PROCHECK v3.5 was used to asses the structural validity of the model (Laskowski et al. 1993).

Thanks to Sarah Nadin for preparation and assay of LpAFP samples and to Dr. Zongchao Jia for helpful discussions. This work was supported by grants from Natural Science and Engineering Research Council of Canada and Canadian Institutes of Health Research (formerly Medical Research Council of Canada) to V.K.W. and P.L.D., respectively.

REFERENCES

Andorfer, C.A., and J.G. Duman. 2000. Isolation and characterization of cDNA clones encoding antifreeze proteins of the Pyrochroid beetle *Dendroides canadensis. J. Insect Physiol* 46:365–372.

Antikainen, M., and M. Griffith. 1997. Antifreeze protein accumulation in freezing tolerant cereals. *Physiologica Plantarum.* 99:423–432.

Bateman, A., A. G. Murzin, and S. A. Teichmann. 1998. Structure and distribution of pentapeptide repeats in bacteria. *Protein Sci* 7:1477–1480.

Baumann, U., S. Wu, K. M. Flaherty, and D. B. McKay. 1993. Three-dimensional structure of the alkaline protease of *Pseudomonas aeruginosa*: a two-domain protein with calcium binding β-roll motif. *EMBO J.* 12:3357–3364.

Chao, H., M. E. Houston Jr, R. S. Hodges, C. M. Kay, B. D. Sykes, M. C. Loewen, P. L. Davies, and F. D. Sönnichsen. 1997. A diminished role for hydrogen bonds in antifreeze protein binding to ice. *Biochemistry.* 36:14652–14660.

Cuff, J. A., M. E. Clamp, A. S. Siddiqui, M. Finlay, and G. J. Barton. 1998. JPred: a consensus secondary structure prediction server. *Bioinformatics.* 14:892–893.

Doucet, D., M. G. Tyshenko, M. J. Kuiper, S. P. Graether, B. D. Sykes, A. J. Daugulis, P. L. Davies, and V. K. Walker. 2000. Structure-function relationships in spruce budworm antifreeze protein revealed by isoform diversity. *Eur. J. Biochem.* 267:6082–6088.

Garnier, J., J. F. Gibrat, and B. Robson. 1996. GOR method for predicting protein secondary structure from amino acid sequence. *Methods Enzymol.* 266:540–553.

Geourjon, C., and G. Deléage. 1995. SOPMA: significant improvements in protein secondary structure prediction by consensus prediction from multiple alignments. *Comput. Appl. Biosci.* 11:681–684.

Graether, S. P., M. J. Kuiper, S. M. Gagne, V. K. Walker, Z. Jia, B. D. Sykes, and P. L. Davies. 2000. β-Helix structure and ice-binding properties of a hyperactive antifreeze protein from an insect. *Nature.* 406: 325–328.

Graham, L. A., Y. C. Liou, V. K. Walker, and P. L. Davies. 1997. Hyperactive antifreeze protein from beetles. *Nature.* 388:727–728.

Gronwald, W., M. C. Loewen, B. Lix, A. J. Daugulis, F. D. Sönnichsen, P. L. Davies, and B. D. Sykes. 1998. The solution structure of type II

antifreeze protein reveals a new member of the lectin family. *Biochemistry.* 37:4712–4721.

Guermeur, Y., C. Geourjon, P. Gallinari, and G. Deléage. 1999. Improved performance in protein secondary structure prediction by inhomogeneous score combination. *Bioinformatics.* 15:413–421.

Haymet, A. D., L. G. Ward, M. M. Harding, and C. A. Knight. 1998. Valine substituted winter flounder "antifreeze": preservation of ice growth hysteresis. *FEBS Lett.* 430:301–306.

Jenkins, J., O. Mayans, and R. Pickersgill. 1998. Structure and evolution of parallel β-helix proteins. *J. Struct. Biol.* 122:236–246.

Jia, Z., C. I. DeLuca, H. Chao, and P. L. Davies. 1996. Structural basis for the binding of a globular antifreeze protein to ice. *Nature.* 384:285–288.

Jones, D. T. 1999. Protein secondary structure prediction based on position-specific scoring matrices. *J. Mol. Biol.* 292:195–202.

Kisker, C., H. Schindelin, B. Alber, J. Ferry, and D. Rees. 1996. A left-handed β-helix revealed by the crystal structure of a carbonic anhydrase from the archaeon *Methanosarcina thermophila. EMBO J.* 15:2323–2330.

Knight, C. A., D. Wen, and R. A. Laursen. 1995. Non-equilibrium antifreeze peptides and the recrystallization of ice. *Cryobiology.* 32:23–34.

Laskowski, R. A, M. W. MacArthur, D. S. Moss, and J. M. Thornton. 1993. PROCHECK: a program to check the stereochemical quality of protein structures. *J. Appl. Cryst.* 26: 283–291.

Levitt, J. 1980. Responses of Plants to Environmental Stress. Chilling, Freezing, and High Temperature Stresses, 2nd ed. Academic Press, New York.

Li, N., B. S. Kendrick, M. C. Manning, J. F. Carpenter, and J. G. Duman. 1998. Secondary structure of antifreeze proteins from overwintering larvae of the beetle *Dendroides canadensis. Arch. Biochem. Biophys.* 360:25–33.

Lilie, H., W. Haehnel, R. Rudolf, and U. Baumann. 2000. Folding of a synthetic parallel β-roll protein. *FEBS Lett.* 47:173–177.

Liou, Y. C., A. Tocilj, P. L. Davies, and Z. Jia. 2000. Mimicry of ice structure by surface hydroxyls and water of a β-helix antifreeze protein. *Nature.* 406:322–324.

Liou, Y. C., P. Thibault, V. K. Walker, P. L. Davies, and L. A. Graham. 1999. A complex family of highly heterogeneous and internally repetitive hyperactive antifreeze proteins from the beetle *Tenebrio molitor. Biochemistry.* 38:11415–11424.

Raymond, J. A., and A. L. DeVries. 1977. Adsorption inhibition as mechanism of freezing resistance in polar fishes. *Proc. Natl. Acad. Sci. U.S.A.* 74:2589–2593.

Rost, B. 1996. PHD: predicting one-dimensional protein structure by profile based neural networks. *Methods Enzymol.* 266:525–539.

Sicheri, F., and D. S. Yang. 1995. Ice-binding structure and mechanism of an antifreeze protein from winter flounder. *Nature.* 375:427–431.

Sidebottom, C., S. Buckley, P. Pudney, S. Twigg, C. Jarman, C. Holt, J. Telford, A. McArthur, D. Worrall, R. Hubbard, and P. Lillford. 2000. Heat-stable antifreeze protein from grass. *Nature.* 406:256.

Sönnichsen, F. D., C. I. DeLuca, P. L. Davies, and B. D. Sykes. 1996. Refined solution structure of type III antifreeze protein: hydrophobic groups may be involved in the energetics of the protein-ice interaction. *Structure.* 4:1325–1337.

Steponkus, P. L., M. Uemura, and M. S. Webb. 1993. A contrast of the cryostability of the plasma membrane of winter rye and spring oat. *In* Advances in Low-Temperature Biology, Vol 2. P.L. Steponkus, editor. JAI Press, London. 211–312.

Thomashow, M. F. 1998. Role of cold-responsive genes in plant freezing tolerance. *Plant Physiol.* 118:1–8.

Tyshenko, M. G., D. Doucet, P. L. Davies, and V. K. Walker. 1997. The antifreeze potential of the spruce budworm thermal hysteresis protein. *Nat. Biotechnol.* 15:887–890.

Urrutia, M. E., J. G. Duman, and C. A. Knight. 1992. Plant thermal hysteresis proteins. *Biochim. Biophys. Acta.* 1121:199–206.

Worrall, D., L. Elias, D. Ashford, M. Smallwood, C. Sidebottom, P. Lillford, J. Telford, C. Holt, and D. Bowles. 1998. A carrot leucine-rich-repeat protein that inhibits ice recrystallization. *Science.* 282:115–117.

Zhang, W., and R. A. Laursen. 1998. Structure-function relationships in a type I antifreeze polypeptide. The role of threonine methyl and hydroxyl groups in antifreeze activity. *J. Biol. Chem.* 273:34806–34812.